Academic Journal of Science and Technology
ISSN: 2771-3032 | Vol. 15, No. 3, 2025

Analysis of Splitting Resistance and Damage Evolution of Fiber Reinforced Concrete Based on Acoustic Emission Parameters

Xingping Hou, Jian Shi, Yi Zhao and Qiyuan Chen

School of Mechanical and Electrical Engineering, Southwest Petroleum University, Chengdu 610000, China

Abstract: Aiming at the splitting resistance and damage process of fiber reinforced concrete, this study uses a universal testing machine and an acoustic emission (AE) system to carry out splitting resistance tests on plain concrete and reinforced concrete containing steel fibers, polypropylene fibers, and cellulose fibers. Load-displacement curves and AE parameters were collected. By analyzing parameters such as load, displacement, ring-down count, average frequency (AF), and rise time/amplitude (RA), the splitting resistance and damage evolution laws of different fiber-reinforced concrete materials were analyzed. The results show that the steel fiber specimen has the highest splitting tensile strength, which is 45.9% higher than that of plain concrete. AE ring-down count shows that the peak ring-down count of the steel fiber specimen is the largest; the duration of the ring-down count of the polypropylene and cellulose specimens is close to that of plain concrete. The proportion of tensile cracks in all specimens is >60%, and the fibers delay the tensile failure by inducing shear energy dissipation. The damage mode of steel fiber concrete changes from interface slip to plastic deformation. Steel fibers significantly improve the ductility of concrete through the bridging effect. This study can provide support for the optimization of engineering structure performance.

Keywords: Fiber Reinforced Concrete; Acoustic Emission Technology; Mechanical Properties; Damage Mechanism; Steel Fiber.

1. Introduction

As one of the most widely used building materials in modern civil engineering, concrete occupies a pivotal position in various construction projects due to its advantages such as good compressive performance, abundant raw material sources, and relatively low cost [1]. However, due to its high brittleness, concrete is prone to brittle fracture when subjected to tensile or impact loads, leading to structural failure. This defect seriously limits the application of concrete in some engineering fields with high requirements for structural performance, such as long-span structures and seismic structures [2].

Fiber reinforcement technology is one of the technical means to improve the performance of concrete. By incorporating various fiber materials into concrete, such as steel fibers, polypropylene fibers, carbon fibers, cellulose fibers, etc. [5], the tensile strength, crack resistance, toughness, and ductility of concrete can be effectively improved. Wei et al.[9] conducted experiments, theoretical analyses, and finite element (FE) modeling to study the effects of fiber content, steel bar ratio, and type on the flexural performance of basalt fiber-reinforced concrete (BFRC) beams, and discussed the flexural behavior of BFRC beams with steel wires or BFRP bars. The results show that a higher steel bar ratio significantly improves the post-crack flexural stiffness and flexural capacity, while increasing the fiber content brings moderate improvements. Wang Weitao et al.[10]produced alumina fiber-reinforced concrete specimens with different alumina fiber lengths and volume contents to explore the effects of alumina fibers on the mechanical properties of concrete, and carried out compressive and flexural performance tests on them. The results show that with the increase in the volume content of alumina fibers, the compressive strength and flexural strength of concrete first gradually increase and then decrease. Hamad et al. [11] tested the mechanical properties and fresh properties of concrete reinforced with four different fibers (PFRC-1, PFRC-2, SFRC-1, and SFRC-2). The analysis shows that among the studied materials, SFRC-2-20 mm-1% (with compressive strength, splitting tensile strength, flexural strength, and workability of 44.7 MPa, 3.64 MPa, 5.3 MPa, and 6.5 cm, respectively) is the most effective combination. The above studies show that different types of fibers and different contents of the same fiber have different effects on the improvement of concrete performance. Therefore, in-depth research on the relationship between fiber type and content and the mechanical properties of concrete is of great engineering significance for optimizing the mix design of fiber-reinforced concrete and improving the performance of concrete structures.

Acoustic emission (AE) technology, as a non-destructive testing technology, can real-time monitor the occurrence and development process of internal damage in materials. When internal damage such as micro-crack initiation and propagation occurs in materials, elastic waves, i.e., acoustic emission signals, will be released. Through the collection, analysis, and processing of acoustic emission signals, characteristic parameters of internal damage in materials can be obtained, such as ring-down count, energy count, average frequency (AF), RA (rise time/amplitude), etc. These parameters can intuitively reflect the degree and type of internal damage in materials [12]. Applying acoustic emission technology to the study of the mechanical properties of fiber-reinforced concrete can deeply understand the evolution law of internal damage in fiber-reinforced concrete during the loading process and reveal the action mechanism of fibers in inhibiting concrete damage.

At present, domestic and foreign scholars have carried out a large number of research works on the mechanical

properties of fiber-reinforced concrete, but most of them focus on traditional mechanical property testing methods, such as compressive strength, tensile strength, flexural strength, etc. [18]. However, the research on systematically analyzing the mechanical properties of fiber-reinforced concrete structures using AE characteristic parameters is relatively scarce. Therefore, carrying out research on the mechanical properties of fiber-reinforced concrete structures based on AE characteristic parameters has important scientific significance and engineering application value.

In this paper, a universal testing machine and an AE system are used to carry out splitting tests on plain concrete and fiber-reinforced concrete cubes containing steel fibers, polypropylene fibers, and cellulose fibers. By analyzing the load-displacement curve and AE parameters, the splitting tensile strength of several fiber-reinforced concretes and the internal damage evolution law during the damage process are studied, providing engineering and technical support for the engineering application of fiber-reinforced concrete.

2. Test Protocol

The test material is a 150×150×150 mm concrete cube provided by the construction unit, as shown in Figure 1. The specimens are divided into four types: plain concrete, steel fiber concrete, polypropylene fiber concrete, and cellulose fiber concrete. Each type of specimen has the same fiber content, and there are three specimens in each group. The universal testing machine is Wance TSE105D, with a maximum load of 500 kN and an accuracy class of 0.5; the test force indication error is 0.5%. The test is carried out according to《GB-T50081-2019 Test Methods for Physical and Mechanical Properties of Concrete》[24].

Figure 1. Concrete cube

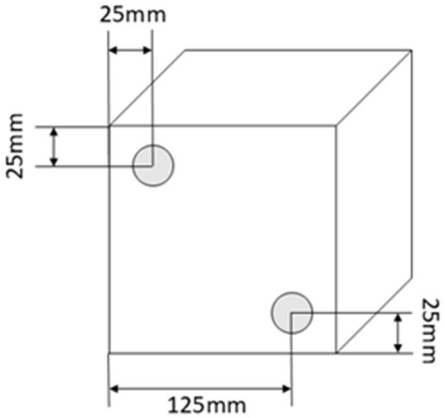

Figure 2. Sensor position

The test is load-controlled loading, and the loading rate is 0.6 MPa/min. The AE system uses the AMSY-6 type acoustic emission system from Vallen Company in Germany, with the AE sensor model VS150-RIC, a sampling frequency of 1 MHz, and a threshold value of 34 dB. The sensor position is shown in Figure 2. Vaseline is used as the couplant between the sensor and the specimen surface, and tape is used to fix it to ensure good signal reception. At the same time, the load and displacement signals of the testing machine are connected to the acoustic emission instrument to ensure the synchronous collection of acoustic emission parameters and load and displacement data.

3. Results and Discussion

3.1. Load-displacement relationship

The load-displacement curves of specimens in each group are shown in Figure 3. The data are tabulated as in Table 1.

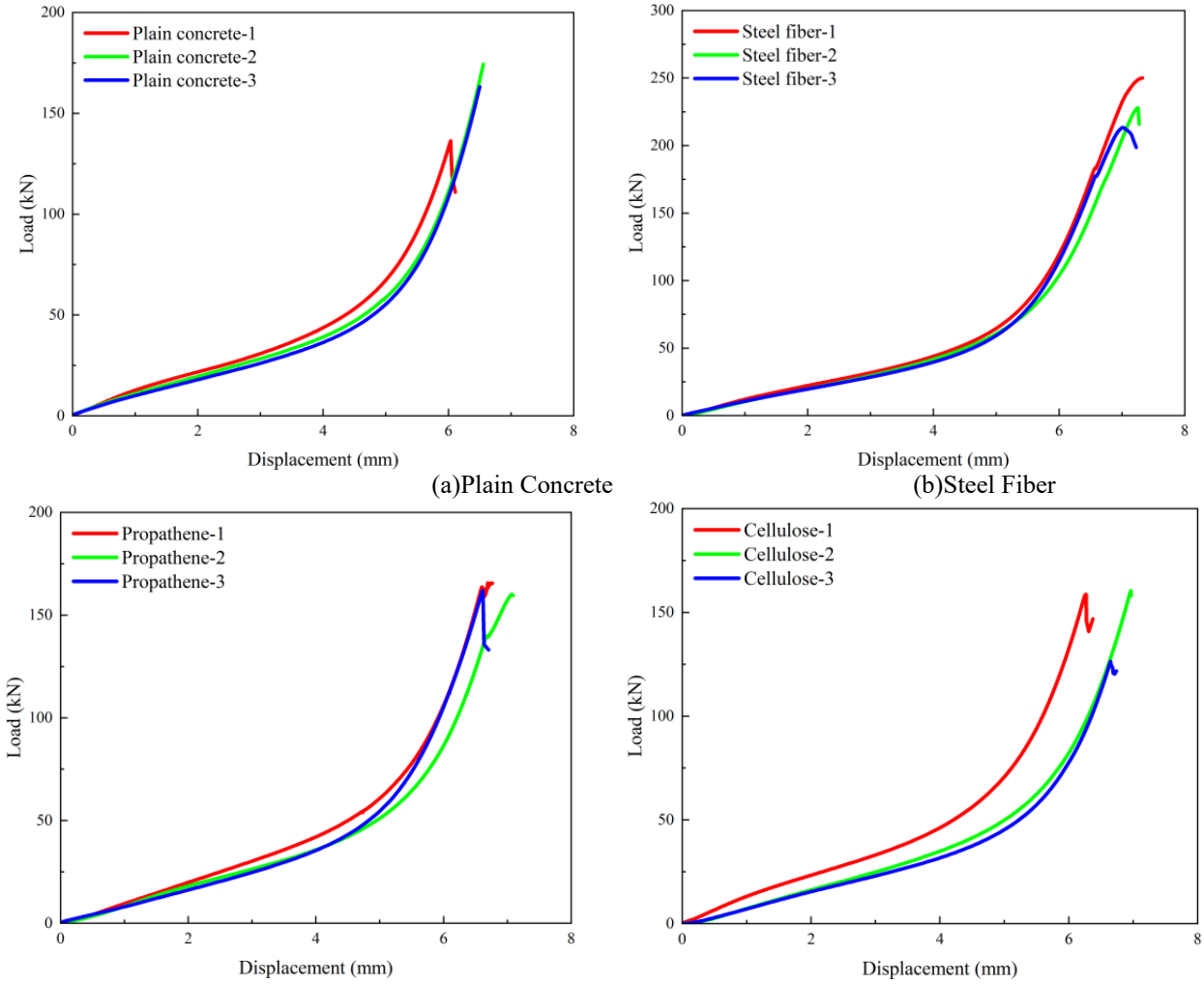

Figure 3. Load-Displacement relationship of specimens in each group

Table 1. Statistics of bearing capacity and tensile strength of specimens in each group

Material	Average Ultimate Bearing Capacity (kN)	Splitting Tensile Strength (MPa)	Strength Change Compared to Plain Concrete
Plain concrete	157.96	4.47	
Steel fiber	230.42	6.52	+45.9%
Prepathene	162.59	4.60	+3%
Cellulose	148.48	4.20	-6%

The results show that when the load is below 50 kN, the change trends of the load-displacement curves of the four types of specimens are basically the same. After the load exceeds 50 kN, the peak load of plain concrete is 157.96 kN, and the load drops sharply after reaching the peak, showing typical brittle failure characteristics. For steel fiber concrete, the peak load reaches 230.42 kN, and the rising section of its curve is steep with large deformation, showing significant ductile failure characteristics, indicating that steel fibers effectively delay crack propagation through the bridging effect and improve the ductility of the material. The polypropylene fiber and cellulose fiber concretes are similar to plain concrete. The peak load of polypropylene fiber is 162.59 kN, with only a 3% increase in strength, and the peak load of cellulose fiber is 148.48 kN, with a 6% decrease in strength compared to plain concrete, indicating that polypropylene fibers and cellulose fibers cannot effectively improve the splitting resistance of the material.

The specimens after the test are shown in Figure 4. The fracture surfaces of plain concrete and cellulose fiber concrete specimens are flat and rough, and the cracks quickly penetrate along the splitting surface without obvious signs of plastic deformation, showing typical brittle tensile failure. The failure forms of steel fiber specimens and polypropylene specimens are mainly surface cracks, but the specimens do not split into two halves, indicating that polypropylene and steel fibers can effectively delay the propagation of cracks.

(a)Plain concrete (b) Steel fiber

(c)Propathene (d) Cellulose

Figure 4. Destruction mode diagrams of each specimen

3.2. Acoustic emission characteristic parameter analysis

3.2.1. Ringing count analysis

Figure 5 shows the relationship between ring-down count, load, and displacement. The AE ring-down count is the number of oscillations exceeding the threshold signal and is the most commonly used acoustic emission characteristic parameter. The ring-down count is simple in form and convenient to process, and can reflect the change trend of the signal, so it is widely used in the activity evaluation of AE.

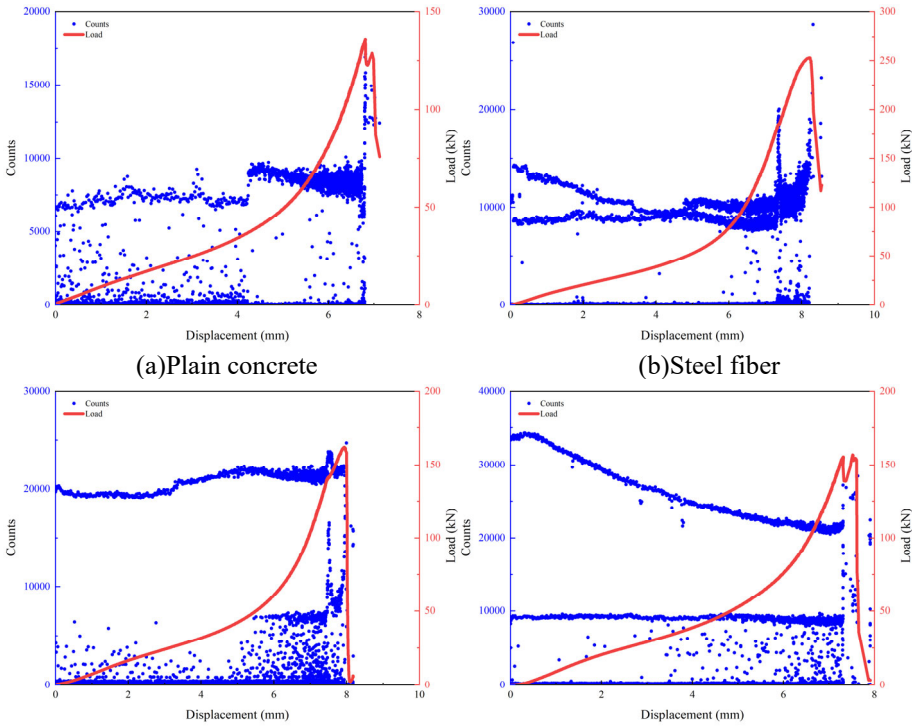

(a)Plain concrete (b)Steel fiber

(c)Propathene (d)Cellulose

Figure 5. Typical specimen ringing count, load and displacement relationship

The results show that the ring-down count is divided into two parts: one is the scattered signal below 10,000 (Type I signal), and the other is the continuously distributed signal exceeding 10,000 (Type II signal). Figure 5-a is a plain concrete specimen with only Type I signals. In Figures 5-c and 5-d, the Type II signals are higher than those in Figure 5-

b, indicating that different fiber materials have different splitting resistances. In the early stage of compression of the plain concrete specimen, the Type I signal is below 10,000; when the load reaches 50 kN, the Type I signal suddenly increases, and the later signal approaches 10,000; finally, when the load reaches the maximum value, the ring-down count increases again. This indicates that in the later stage of the test, the plain concrete specimen undergoes rapid crack initiation and penetration under tensile stress, and energy is concentrated and released at the moment of failure. Due to the lack of effective inhibition of crack propagation by fibers, the ring-down count only reflects the single fracture process of the matrix.

The Type I signal of the steel fiber specimen has the same trend as that of the plain concrete Type I signal; the early stage of the Type II signal shows a gradually decreasing trend, with a difference of about 2,000 from the maximum value of the Type I signal. When the load reaches 50 kN, the Type II signal tends to be gentle, basically the same as the value of the Type I signal; the later signal gradually increases, and the peak approaches 25,000 times. This indicates that in the steel fiber concrete specimen, due to the different elastic moduli of steel fibers and plain concrete, two types of signals are generated; in the early stage of loading, with the increase in elastic deformation, the deformation of steel fibers is greater than that of plain concrete; with the increase in load, the steel fibers gradually enter the yield stage, and the deformation of steel fibers is basically the same as that of plain concrete. At this time, interface slip occurs between the steel fibers and the plain concrete matrix, and crack propagation is hindered, reflecting a multi-stage energy dissipation process of "crack propagation-fiber slip-plastic deformation"; in the later stage of loading, due to the micro-crack propagation in plain concrete, the steel fibers are gradually pulled out and fractured, and both Type I and Type II signals increase until the specimen fractures.

The Type II signal of the polypropylene fiber specimen is higher than that of the steel fiber, with a peak of about 22,000 times, and also higher than that of plain concrete. During the loading process, it shows a "platform" change trend. This is because the polypropylene fiber has a low elastic modulus and low strength, and is easily broken under load. The high-frequency acoustic emission signal released at the moment of fracture leads to a high peak ring-down count; at the same time, the weak bonding between the fiber and the matrix has little effect on the splitting resistance of plain concrete.

The Type II signal of the cellulose fiber specimen is higher than that of the steel fiber and polypropylene fiber, with a peak of about 40,000 times, and also higher than that of plain concrete. During the loading process, it shows a decreasing change trend. This is because the elastic modulus of cellulose fiber is much lower than that of steel fiber and polypropylene fiber, and it has poor compatibility with plain concrete and weak interface bonding. A large number of debonding or brittle fractures occur in the early stage of loading, releasing a large number of high-frequency signals; after the fiber fractures with the increase in load, it not only cannot hinder the crack propagation but may also become a new crack source, accelerating the matrix failure.

3.2.2. Cumulative Energy Analysis

Cumulative energy is the accumulated value of acoustic emission signal energy, which reflects the total amount and rate of energy release during material damage and, together with parameters such as load-displacement curves and ring-down counts, reveals the failure characteristics of fiber concrete. Figure 6 shows the relationship between the cumulative energy, load, and displacement of each specimen.

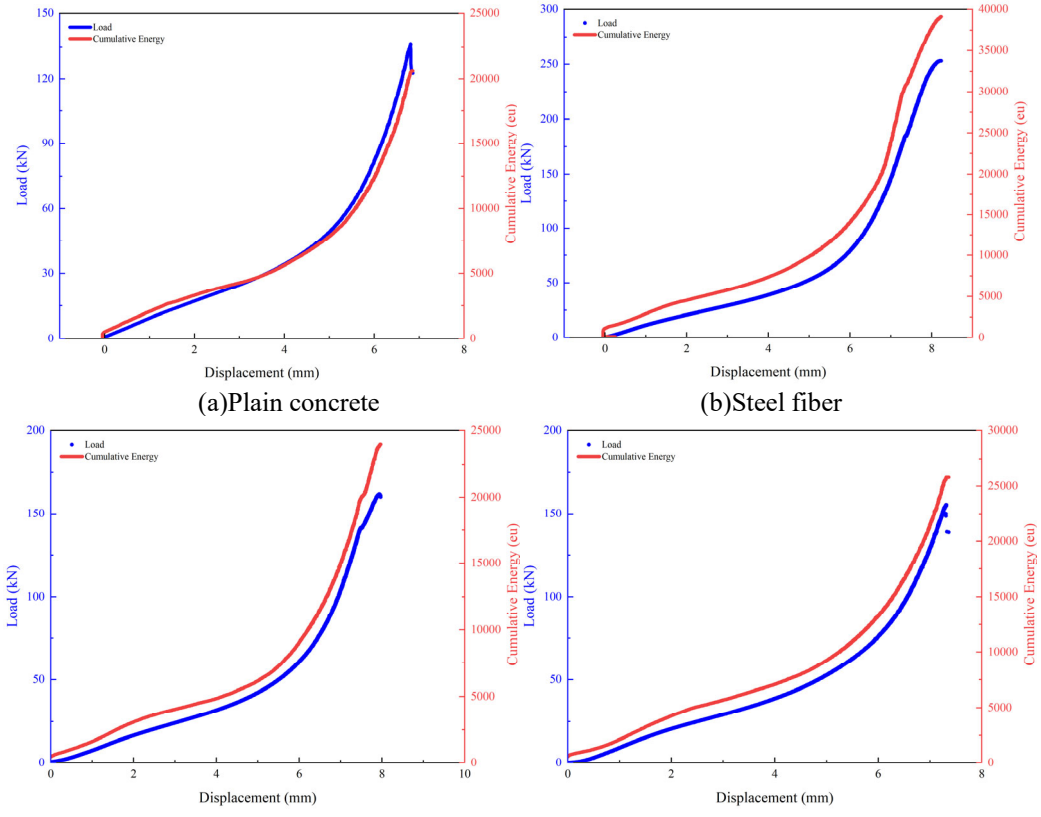

(a)Plain concrete (b)Steel fiber

(c)Propathene (d)Cellulose

Figure 6. Cumulative Energy - Energy - Load and Displacement Relationship Diagram

The results show that the change trend of cumulative energy is basically the same as that of load. The change in cumulative energy of each specimen is divided into two stages: when the load is less than 50 kN, the cumulative energy increases slowly; after 50 kN, the cumulative energy increases rapidly and reaches the peak at fracture. Compared with the cumulative energy of brittle failure plain concrete, the cumulative energy of steel fiber concrete is the highest, indicating that the specimen continuously dissipates energy throughout the cycle from micro-crack initiation-fiber slip-plastic deformation, corresponding to significant displacement ductility and strength improvement. The maximum cumulative energy of the polypropylene fiber specimen is close to that of the plain concrete specimen and lower than that of the steel fiber specimen, indicating that the energy mainly comes from the deformation of plain concrete; the cumulative energy of the cellulose fiber specimen changes the same as that of the polypropylene specimen, indicating that the splitting resistance of polypropylene and cellulose fiber specimens is lower than that of steel fiber specimens.

3.2.3. RA-AF association analysis

Japan Concrete Association connects AF(average frequency) and RA(rise time/amplitude) parameters to evaluate the crack failure mechanism of concrete materials[25]. The calculation method of AF and RA parameters is as follows:

$$AF = \text{Acoustic emission count/duration}$$

$$RA = \text{Rise time/amplitude}$$

It is found that the stretched AE signal is distributed with high AF and low RA, while the shear AE signal is distributed with low AF and high RA, as shown in Fig 7. The JCMS-IIIB5706 (2003) standard defines an Angle of 45° as the dividing line between tensile crack and shear crack. The tensile crack near AF crack is the tensile crack, and the shear crack near RA crack is the shear crack, and the slope AF/RA of the straight line is called the threshold value of tensile crack judgment, as shown in Fig 7. The damage crack identification method based on acoustic emission AF-RA parameters is widely used in engineering[26].

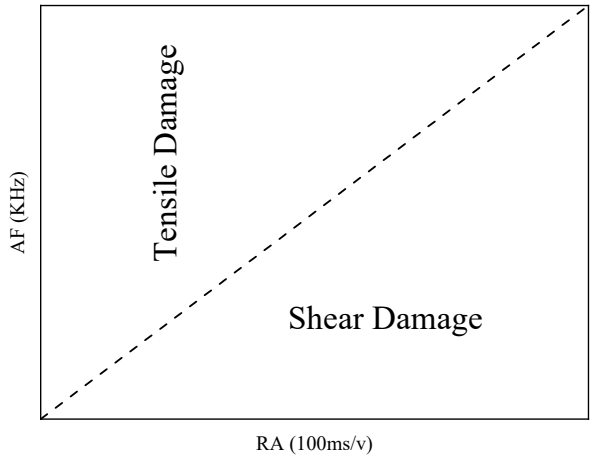

Figure 7. Schematic diagram of RA-AF correlation analysis

In this study, the boundary inflection point method was used to determine the critical point k_0 of the boundary slope k[31]. The boundary inflection point method is an algorithm based on calculating the maximum curvature to identify inflection points on curves, characterized by its ability to automatically recognize inflection points on data curves quickly and effectively without manual marking. This method was applied to analyze the acoustic emission parameters of representative specimens. Within the range of natural numbers k from 0 to 1000, the inflection point position , the optimal slope k_0 was selected at the point of maximum curvature on the curve by calculating the curvature formula according to the variation of shear damage proportion with boundary slope k. Table 2 presents the results of the optimal slope k_0 values for the specimens.

Table 2. Calculate the optimal slope k0 for each typical specimen.

Specimen	Plain concrete	Steel fiber	Propathene	Cellulose
Optimal Slope k0	11	22	20	7

As shown in Figure 8 is the tensile-shear damage classification diagram of each specimen. Statistics show that the proportion of tensile cracks in plain concrete, polypropylene, and cellulose specimens exceeds 80%, indicating that these three types of specimens are mainly subjected to tensile stress in the concrete matrix, resulting in brittle fracture. The proportion of tensile cracks in steel fiber specimens is 62.4%, far lower than that in plain concrete, polypropylene, and cellulose specimens, indicating that due to the presence of steel fibers, the shear cracks caused by shear stress generated during the deformation of the specimen due to fiber-matrix interface slip and fiber plastic deformation increase in proportion, causing the damage mode to change from "brittle tension" to "ductile shear".

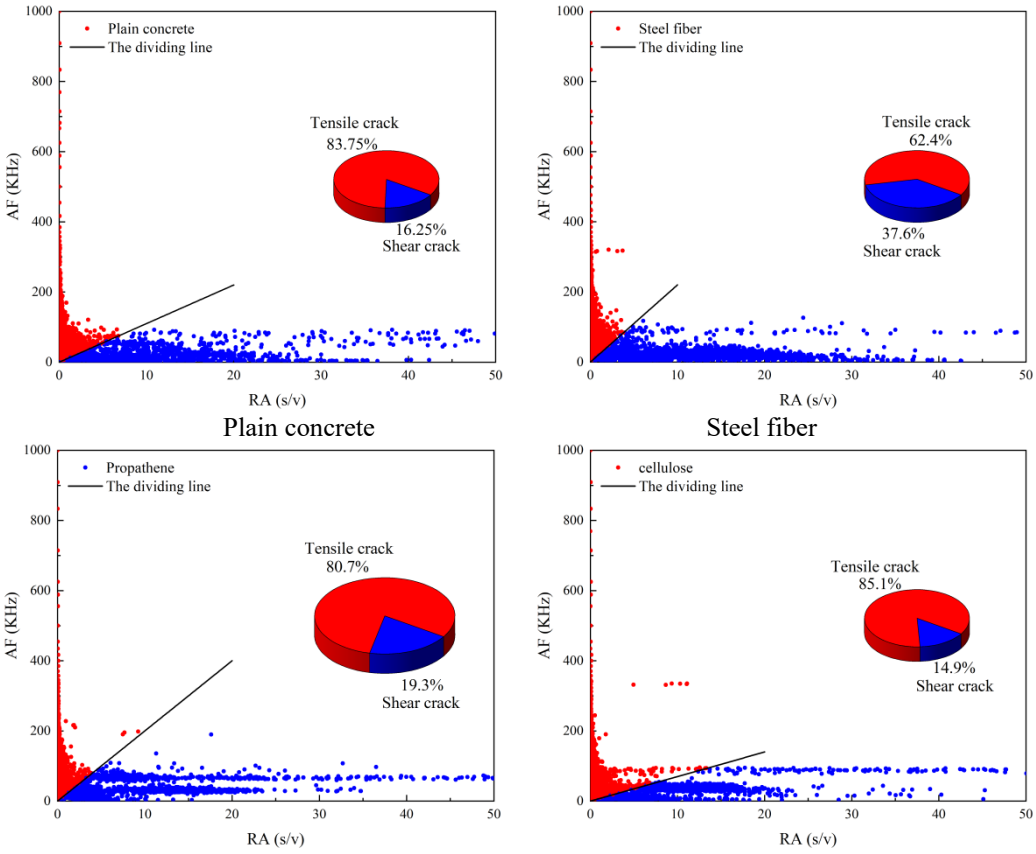

Figure 8. Tensile-shear damage classification

4. Summary

In this study, the splitting resistance of different fiber concrete cube specimens was studied using acoustic emission characteristic parameters. Through the analysis of load-displacement curves, AE ring-down counts, cumulative energy, and RA and AF characteristic parameters, the following conclusions were obtained:

1.Steel fiber concrete has the best splitting resistance, with an average splitting tensile strength of 6.52 MPa, which is 45.9% higher than that of plain concrete specimens (4.47 MPa); polypropylene and cellulose fibers have no obvious effect on the splitting resistance of concrete.

2.The change trends of AE ring-down counts and cumulative energy reflect the different damage changes between steel fiber, polypropylene, cellulose specimens, and plain concrete. Steel fiber concrete is dominated by micro-crack initiation-fiber slip-plastic deformation-ductile fracture; polypropylene and cellulose specimens are dominated by micro-crack initiation-fiber fracture-brittle fracture; plain concrete is dominated by brittle fracture.

3.The proportion of tensile cracks in the four materials is >60%, and the presence of shear is due to the shear stress generated by fiber-matrix interface slip; steel fibers cause a high proportion of shear cracks through the "bridging-pull-out" mechanism, which can delay tensile failure; while polypropylene fibers and cellulose fibers have a low proportion of "bridging-pull-out", resulting in a low proportion of shear cracks.

References

[1] Zhang Yuan. Research on the Preparation and Properties of Nano - Carbon Fiber Cement - based Composites [D]. Dalian University of Technology, 2014.

[2] Wu Kai, Liu Xiaoyi, Chen Feng, et al. Study on the Interface Failure Mechanism of Steel-Steel Fiber Reinforced Concrete Composite Structures under Different Load Conditions [J]. Engineering Mechanics, 2021, 38(2): 110-121.

[3] Yue Jianguang, Xia Yuefei, Fang Hua. Experimental Study on the Fracture Mechanism and Tensile Damage Constitutive of Steel Fiber Reinforced Concrete [J]. China Civil Engineering Journal, 2021, 54: 93-106.

[4] Wang Zhaoyao. Study on the Mechanical Properties of Steel Fiber Reinforced Concrete Beams Based on the Fiber Pull-Out Mechanism [D]. Tianjin University, 2022.

[5] Lolla, SrilakshmiCAa,Oinam,et al. Tensile strength and flexural behavior of steel fiber-reinforced concrete beams[J]. Structural Concrete,2025,Vol.26(1): 501-530.

[6] Sergii Kroviakov,Vitalii Kryzhanovskyi,Daria Hedulian. Comparison of the Corrosion Resistance of Fiber-Reinforced Concrete with Steel and Polypropylene Fibers in an Acidic Environment[J]. Construction Materials,2025,Vol.5(1): 6.

[7] Kumbhar A. N,Kadam S. S. TITLE: EXPERIMENTAL INVESTIGATION OF MIXED FIBER REINFORCED CONCERETE DEEP BEAM IN SHEAR[J]. International Journal of Engineering Research and General Science, 2015, Vol.3.

[8] Xiaofei Liu,Xin ZhouCA1,Xiaoran Wang,et al. Time-varying damage evolution of concrete under cyclic disturbance loading-an experimental observation utilizing AE and DIC[J]. Case Studies in Construction Materials,2024,Vol.20: e03219.

[9] Wang Weitao, Hong Gang, He Shengwen, et al. Experimental Study on the Mechanical Properties of Alumina Fiber - Reinforced Concrete [J]. Modern Chemical Industry, 2024, 44(201): 124-128.

[10] Khalel, Hamad Hasan Zedan CAa, Khan, et al. Parametric Study for Optimizing Fiber-Reinforced Concrete Properties [J]. Structural Concrete, 2025, Vol. 26(1): 88-110.

[11] Kumbhar A. N, Kadam S. S. TITLE: EXPERIMENTAL INVESTIGATION OF MIXED FIBER REINFORCED CONCERETE DEEP BEAM IN SHEAR [J]. International Journal of Engineering Research and General Science, 2015, Vol. 3.

[12] Yang Qing Dynasty, LI Pengnan, Qiu Xinyi, et al. Pore exit delamination damage identification of carbon fiber composites based on acoustic emission [J]. Aerospace Materials Technology,2023,53(5): 90-96.

[13] Pan Tambo, ZHENG Yonglai, Xu Xubing, et al. Characteristics of damage and cracks of corroded concrete beams under bending monitoring by acoustic emission [J]. Journal of Tongji University (Natural Science), 2024,52(3): 350-359

[14] Ye Tian;Duo LiuCA1;Xudong Chen; et al.Damage evolution of steel-UHPC composite beams using AE and DIC techniques [J]. Journal of Constructional Steel Research, 2025,Vol.224: 109163

[15] Świt, GrzegorzCAa;Dzioba, Ihor R.CAb;Adamczak-Bugno, AnnaCAc; et al.Identification of the Fracture Process in Gas Pipeline Steel Based on the Analysis of AE Signals [J]. Materials, 2022, Vol.15(7): 2659

[16] Świt, GrzegorzCAa;Dzioba, Ihor R.CAb;Adamczak-Bugno, AnnaCAc; et al.Identification of the Fracture Process in Gas Pipeline Steel Based on the Analysis of AE Signals [J]. Materials, 2022, Vol.15(7): 2659

[17] Wang Weitao, Hong Gang, He Shengwen, et al. Experimental Study on the Mechanical Properties of Alumina Fiber - Reinforced Concrete [J]. Modern Chemical Industry, 2024, 44(S1): 124 - 128.

[18] Guo Yihang, Li Li, Yang Chenxin, et al. Research Progress on Plant Fiber - Reinforced Concrete [J]. Bulletin of the Chinese Ceramic Society, 2022, 41(10): 3347 - 3358.

[19] Gong Mingzi, Pan Axin, Zhang Zilong, et al. Research on the Pull - out Behavior of Steel Fibers in Ultra - High - Performance Fiber - Reinforced Concrete [J]. Bulletin of the Chinese Ceramic Society, 2023, 42(8): 2764 - 2772.

[20] Khalel, Hamad Hasan ZedanCAa,Khan,et al. Parametric study for optimizing fiber-reinforced concrete properties[J]. Structural Concrete,2025,Vol.26(1): 88-110.

[21] Hogr Z. Hassan & Najmadeen M. Saeed. Fiber reinforced concrete: a state of the art[J]. Discover Materials,2024,Vol.4(1): 1-44.

[22] ZhiWei Wei,TongShuai Wang,HongJie Li,et al. Study of the flexural behavior of basalt fiber-reinforced concrete beams with basalt fiber-reinforced polymer bars and steel bars[J]. Case Studies in Construction Materials,2025,Vol.22: e04433.

[23] de Almeida, Ricardo Laguardia JustenCAa,Parsekian,et al. Investigation on the flexural behavior of high-strength fiber-reinforced concrete[J]. Structural Concrete,2025,Vol.26(1): 365-384.

[24] Standard for Test Methods of Concrete Physical and Mechanical Properties: GB/T 50081 - 2019 [S]. Ministry of Housing and Urban - Rural Development of the People's Republic of China; State Administration for Market Regulation, 2019 - 06 - 19.

[25] Ming Lan,Yan He,Chunlong Wang, et al.Fractal evolution characteristics of fracture meso-damage in uniaxial compression rock masses using bonded block model [J]. Scientific reports, 2024, Vol.14(1): 17979

[26] Guan Qingyuan. Acoustic emission multi-parameter analysis and damage recognition of reinforced concrete beam damage process [D].null,2023

[27] Jianchun Ou;Enyuan WangCA1;Xinyu Wang; et al.Acoustic emission characteristics and damage evolution of different rocks under uniaxial compression conditions[J].Scientific Reports, 2024,Vol.14(1): 4179

[28] Xianhui Feng;Huilin LiuCA1;Xu Chen; et al.Acoustic emission characteristics and cracking mechanism analysis of anisotropic shale containing a circular hole under uniaxial compression [J]. Theoretical and Applied Fracture Mechanics, 2025, Vol.135: 104771

[29] Wei Shen;Hao Bai;Fei Wang; et al.Acoustic Emission characteristics and damage evolution of Concrete-Encased CFST columns under compressive load[J].Engineering Fracture Mechanics,2024,Vol.311: 110578

[30] Zhang, XC (Zhang, Xinchen);Shan, WC (Shan, Wenchen);Zhang, ZW (Zhang, Zhongwen); et al.AE monitoring of reinforced concrete squat wall subjected to cyclic loading with information entropy-based analysis [J]. Engineering Structures,2018,Vol.165: 359-367

[31] WANG Juxian, LIANG Peng, ZHANG Yanbo, et al. Research on rock tensile shear fracture classification based on acoustic emission RA-AF value and kneedle algorithm [J]. Chinese Journal of Rock Mechanics and Engineering, 2018,43(201): 3267-3279